ELSEVIER

International Journal of Mass Spectrometry 176 (1998) 227–235

International Journal of Mass Spectrometry

Application of ab initio direct dynamics calculations on the ionization and electron attachment processes for the CCl_3F molecule

Toshiyuki Takayanagi[a],*, Yuzuru Kurosaki[a], Hiroto Tachikawa[b]

[a]*Advanced Science Research Center, Japan Atomic Energy Research Institute, Tokaimura, Ibaraki-ken 319-1106, Japan*
[b]*Division of Molecular Chemistry, Graduate School of Engineering, Hokkaido University, Sapporo 060-8628, Japan*

Received 6 February 1998; accepted 10 April 1998

Abstract

Ab initio direct dynamics calculations have been carried out for the ionization and electron attachment processes for the CCl_3F molecule in order to obtain dynamical information on these processes. CCl_3F^+ produced via vertical ionization directly dissociates into $CCl_2F^+ + Cl$ within a very short time. It has been found that 80% of the available energy is partitioned into the relative translational energy. It has been also found that CCl_3F^- formed by vertical electron attachment dissociates to $CCl_2F + Cl^-$; however, the energy partitioning was very different from the CCl_3F^+ case. This difference in the dissociation dynamics has been discussed on the basis of the potential energy curves. (Int J Mass Spectrom 176 (1998) 227–235) © 1998 Elsevier Science B.V.

Keywords: Ab initio calculations; Direct dynamics; Ionization; Electron attachment; Potential energy surface

1. Introduction

The classical trajectory method has been a convenient and powerful tool for understanding chemical reaction dynamics. In a traditional approach, classical trajectories are calculated on an analytical potential energy surface, which is generally constructed by a fit to potential energies obtained from ab initio molecular orbital (MO) calculations for a large number of geometrical configurations. However, it is still difficult to apply such a procedure to general polyatomic reaction systems because of a large number of degrees of freedom. An alternative approach, on the other hand, is to calculate the classical trajectories directly utilizing the ab initio MO method without construction of the potential energy surface. Due to recent advances in computer hardware as well as the development of efficient ab initio computational codes, this method has become feasible in recent years. In fact, the ab initio direct dynamics method has already been applied to various reaction systems [1–12]. The disadvantage of this method is that it generally requires a large CPU time to generate even one trajectory and thus it is not feasible to calculate a large number of trajectories for obtaining statistical quantities such as cross sections and energy distributions. In spite of this limitation, it should be emphasized that the direct use

---

* Corresponding author. E-mail: tako@popsvr.tokai.jaeri.go.jp

PII S1387-3806(98)14036-8

of the ab initio MO results in the trajectory calculations is very convenient in order to understand the reaction dynamics because a typical trajectory generally gives dynamical information such as kinetic energy release, typical reaction time, and so on. In this paper we present ab initio direct dynamics calculations for the ionization and dissociative electron attachment processes for the CCl_3F molecule.

In the previous paper [9] we have theoretically studied the mechanism and dynamics of the ionization and dissociative electron attachment processes of CCl_4 using the ab initio MO theory combined with the ab initio direct dynamics calculations. Two important conclusions were obtained from our previous work. The first is that the CCl_4^+ cation produced by vertical ionization spontaneously dissociates into CCl_3^+ and Cl; the typical dissociation time is about 0.1 ps. The second is that the CCl_4^- anion formed via vertical electron attachment does not dissociate into CCl_3 and Cl^- within 0.6 ps and vibrationally excited CCl_4^- is produced despite the fact that such a dissociation process is energetically possible. We here extend our previous work to the CCl_3F molecule and compare to the results for the CCl_4 molecule.

Although the CCl_3F molecule is simple and is also important in the chemistry of the upper atmosphere, very few ab initio MO studies, especially on its charged species, have been reported so far. Peyerimhoff and Buenker [13] carried out pioneering work on the potential energy surfaces (PES) of CCl_3F^+ and CCl_3F^- using the ab initio multireference-double-configuration-interaction (MRDCI) method. They have obtained the limited potential curves as a function of one of the C–Cl distances in CCl_3F. Their computational result shows that the lowest two states of CCl_3F^+ are nearly degenerate and the ionization potentials calculated for these two states are in good agreement with experimental values. The result for CCl_3F^- also shows that electron attachment to the CCl_3F molecule leads to dissociation into the $CCl_2F + Cl^-$ channel and is qualitatively consistent with the electron attachment experiments in the gas phase. Lunell and co-workers [14] later studied the electronic structure of CCl_3F^+ at the less accurate Hartree–Fock (HF)/3–21G* level of theory. They found that the CCl_3F^+ cation dissociates into CCl_2F^+ and Cl. This result is qualitatively consistent with photoionization experiments [15] in the gas phase; however, the detailed potential energy surfaces have not been calculated. Gustev [16] have recently employed a local spin density functional approximation to calculate the electron affinity of CCl_3F. Therefore, information on the detailed mechanism and dynamics of the electron attachment and ionization processes for the CCl_3F molecule is still insufficient.

The purpose of the present study is to obtain information on the dynamical properties of the charged CCl_3F molecule produced by the electron attachment or ionization process: a dissociation time, energy partitioning of fragments, and so on. These properties give important information on the dynamical behaviors of charged molecules not only in the gas phase but also in the condensed phase.

2. Method of calculations

All ab initio MO calculations were carried out using the GAUSSIAN 94 program [17]. Most of the calculations were carried out at the HF level of theory using the correlation consistent polarized valence double-zeta (cc-pVDZ) basis set of Dunning [18]. In order to study the effect of electron correlation, coupled-cluster with single double substitution (CCSD) calculations were done with the geometries optimized at the HF level. The effect of diffuse function was also examined by changing the basis set into the augmented cc-pVDZ (aug-cc-pVDZ) basis.

In the present article, the classical trajectory calculations were carried out directly using the ab initio MO results without constructing an analytic potential energy surface function. Classical equations of motion were numerically solved by the standard fourth-order predictor–corrector method. An ab initio MO calculation was done at every step of the trajectory calculation using the GAUSSIAN 94 program. We employed the HF/cc-pVDZ optimized geometry of the neutral CCl_3F molecule as an initial structure of the trajectory calculations. Initial atomic velocities were randomly selected so as to give a sufficiently

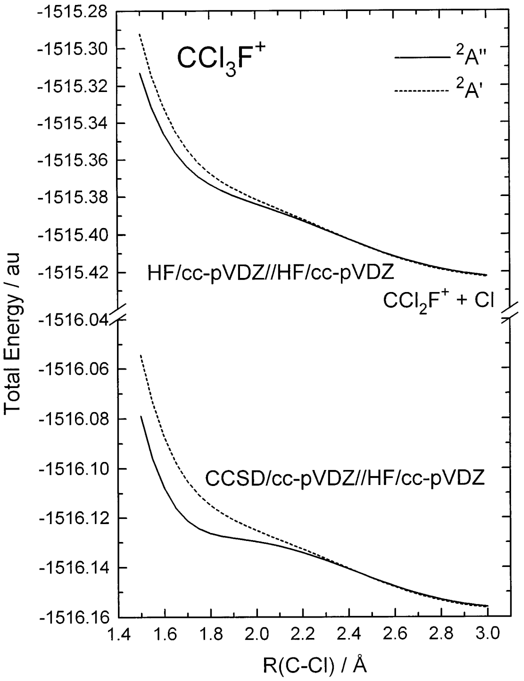

Fig. 1. Potential energy curves for CCl_3F^+ as a function of one of the C–Cl distances. Upper two curves were calculated at the HF/cc-pVDZ level while lower two curves were obtained at the CCSD/cc-pVDZ level. The other internal coordinates are optimized at the HF/cc-pVDZ level of theory.

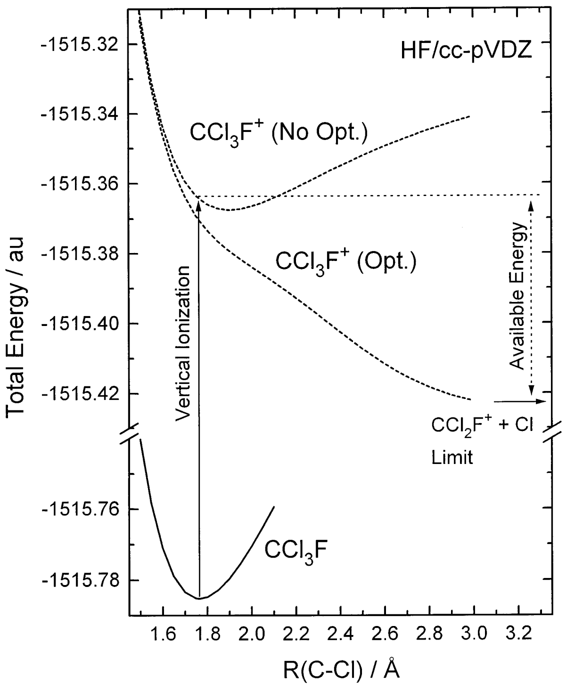

Fig. 2. A schematic description of vertical ionization of CCl_3F. Potential curves are calculated at the HF/cc-pVDZ level. “Opt” means that the internal coordinates other than the one C–Cl distance are optimized. “No opt” means that the internal coordinates other than the one C–Cl distance are fixed to those of the neutral CCl_3F minimum.

small center-of-mass kinetic energy (typically less than 0.1 kcal/mol). Note that zero-point vibrational energies were completely ignored in the present calculations. The trajectory calculations were done at the HF/cc-pVDZ level of theory with the analytical gradient technique.

3. Results and discussion

3.1. CCl_3F^+ cation

Fig. 1 shows the potential energy curves for the lowest two states of CCl_3F^+, $^2A''$ and $^2A'$, calculated at the HF/cc-pVDZ level of theory as a function of one of the three C–Cl distances. Other geometric parameters are fully optimized in this figure. It is seen that both the $^2A''$ and $^2A'$ states are nearly degenerate although the $^2A''$ state is slightly lower than the $^2A'$ state at smaller C–Cl distances. The present results are qualitatively consistent with the MRDCI results by Peyerimhoff and Buenker [13]. It is also seen that the potential curves for CCl_3F^+ are completely repulsive. In order to examine the effect of electron correlation, the potential energy curve was calculated at the CCSD/cc-pVDZ level for the HF/cc-pVDZ optimized geometries. The result is also plotted in Fig. 1 and is found to be very similar to the HF/cc-pVDZ result. This suggests that the classical trajectory calculations at the HF/cc-pVDZ level would give a qualitatively accurate description of the dissociation dynamics of the CCl_3F^+ cation.

Before we present the classical trajectory results, the vertical ionization process of CCl_3F is schematically described in Fig. 2. The potential energy curves calculated at the HF/cc-pVDZ level are plotted as a function of one of the C–Cl distances. The solid line indicates the potential curve for the neutral CCl_3F molecule. The lower dashed curve indicates the $^2A''$ potential for which other geometrical parameters are optimized. The upper dashed curve shows, on the other hand, the potential curve in which the other geometrical parameters are fixed to those of the neutral CCl_3F molecule. The comparison of these two curves clearly indicates the effect of geometrical optimization is significant at larger C–Cl distances. In other words, the molecular geometries of the CCl_2F^+ moiety are quite different between small C–Cl distances and large C–Cl distances. In fact, the asymptotic CCl_2F^+ molecule has a planer C_{2v} structure. Therefore, it is expected that a part of the available energy is partitioned into the vibrational energy of the CCl_2F^+ fragment in the dissociation of CCl_3F^+. The available energy was calculated to be 36 kcal/mol at the HF/cc-pVDZ level of theory.

The result of the classical trajectory calculation is depicted in Fig. 3. Fig. 3(a) shows the potential energy as a function of reaction time, while the nuclear distances are plotted as a function of time in Fig. 3(b). In this calculation, the initial condition was determined so as that the molecular geometries are constrained within C_s symmetry. Also, only the $^2A''$ potential surface was considered since the characteristics of the $^2A'$ surface was found to be very similar to that of the $^2A''$ surface. It is seen that the potential energy suddenly decreases in a very short time region 0–0.04 ps. This behavior is due to the repulsive nature of the $^2A''$ potential surface in the Franck–Condon region. On the other hand, one of the C–Cl distances gradually and monotonously increases. This clearly shows that vertical ionization leads to spontaneous dissociation of CCl_3F^+ into the CCl_2F^+ + Cl channel. The relative translational energy between the CCl_2F^+ and Cl fragments was estimated to be 28 kcal/mol from this trajectory result. This means that 79% of the available energy is partitioned into the relative translational energy and 21% is partitioned into mostly the vibrational energy of the CCl_2F^+ fragment. Although we did not analyze the vibrational modes in detail, Fig. 3(c) qualitatively suggests that the out-of-plane bending mode of CCl_2F^+ is considerably excited. These results strongly suggest that the dissociation dynamics cannot be predicted by statistical theories [19].

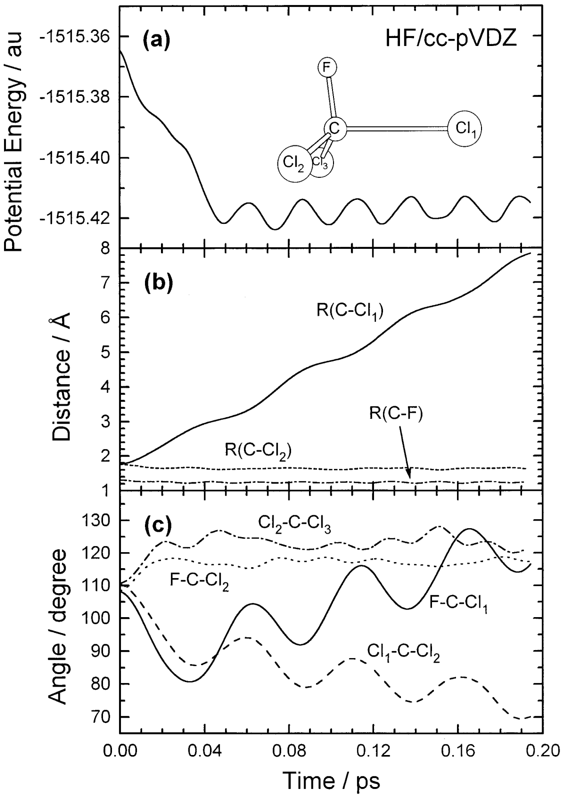

Fig. 3. The result of the classical trajectory calculation for CCl_3F^+ formed by vertical ionization: (a) potential energy, (b) internuclear distances, and (c) bending angles as a function of time.

It should also be informative to compare the present theoretical results to available experimental data. Photoion–photoelectron coincidence (PIPECO) spectroscopy [19] is one of the experimental methods by which energy distributions of dissociation fragments can be obtained; however, no such experimental data are available for the CCl_3F molecule, as far as we are aware.

3.2. CCl_3F^- anion

Fig. 4 shows the potential energy curve for CCl_3F^- calculated at the HF/cc-pVDZ level of theory (solid line) as a function of one of the three C–Cl distances. Other geometric parameters are fully optimized. It can

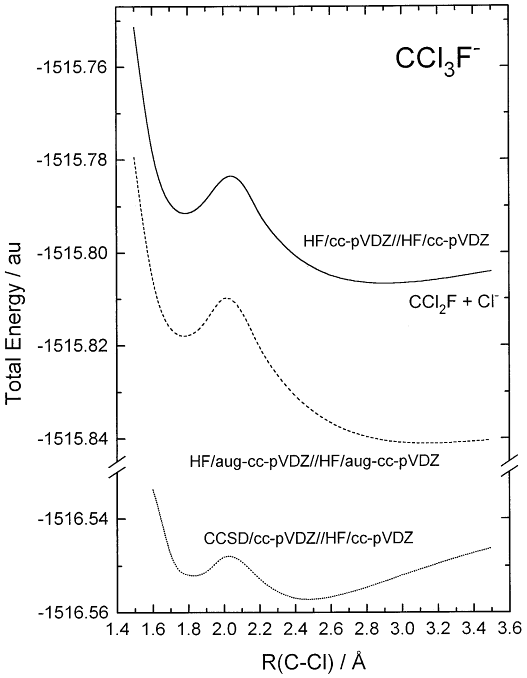

Fig. 4. Potential energy curves for CCl_3F^- as a function of one of the C–Cl distances. Upper two curves were calculated at the HF/cc-pVDZ level while the lower curve was obtained at the CCSD/cc-pVDZ level. The other internal coordinates are optimized at the HF/cc-pVDZ level of theory.

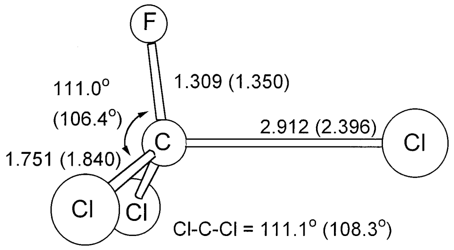

(a) $CCl_3F^-(C_s)$

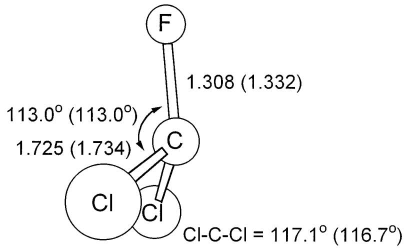

(b) CCl_2F (C_s)

Fig. 5. Molecular geometries of (a) the elongated CCl_3F^- structure and (b) the asymptotic CCl_2F fragment optimized at the HF/cc-pVDZ level of theory. Numbers in parentheses are the values optimized at the MP2(fc)/cc-pVDZ level (bond lengths in Å, angles in degree).

be seen that the potential curve has two local minima at short and long C–Cl distances. These two structures correspond to a compressed structure and an elongated structure, as was found in the case of the CCl_4^- anion [9]. Note that the elongated structure is more stable than the compressed structure. The effect of inclusion of diffuse basis set was examined by changing the basis set into aug-cc-pVDZ. The result is also plotted in Fig. 4 as a dashed line. The inclusion of the diffuse basis function does not largely affect the characteristic of the potential curve although the decrease in total electronic energy is more significant at larger C–Cl distances. The effect of electron correlation was also examined at the CCSD/cc-pVDZ level of theory. It is found that the elongated structure becomes more stable with respect to the asymptotic $CCl_2F + Cl^-$ energy level. Also, the location of the minimum corresponding to the elongated structure shifts to a smaller C–Cl distance.

Fig. 5 shows the molecular geometry of the elongated CCl_3F^- structure determined at the HF/cc-pVDZ level of theory. Also shown in Fig. 5 is the molecular structure of the asymptotic CCl_2F radical. It can be seen that the structure of the CCl_2F moiety in CCl_3F^- is very similar to that of the CCl_2F radical. This suggests that the elongated CCl_3F^- structure is essentially a charge-dipole type complex, $Cl^- \cdots CCl_2F$. In fact, a simple Mulliken analysis shows that most of the negative charge in CCl_3F^- is localized on the elongated Cl atom; the value was calculated to be 0.92 at the HF/cc-pVDZ level of theory. Table 1 also reports harmonic vibrational frequencies for CCl_3F^- and CCl_2F calculated at the HF/cc-pVDZ level. It is interesting to note that the elongated CCl_3F^- anion has a very loose structure because of very low vibrational frequencies. We have also optimized the geometries for CCl_3F^- and CCl_2F at the MP2(fc)/cc-pVDZ level of theory in order to

Table 1
Harmonic vibrational frequencies for CCl_3F^- and CCl_2F calculated at the HF/cc-pVDZ and MP2(fc)/cc-pVDZ levels of theory

Symmetry	Frequency/cm^{-1}
CCl_3F^- (Cs) at HF/cc-pVDZ	
a'	75, 100, 300, 485, 627, 1285
a''	44, 406, 931
CCl_3F^- (Cs) at MP2(fc)/cc-pVDZ	
a'	131, 197, 266, 429, 571, 1074
a''	57, 345, 722
CCl_2F (Cs) at HF/cc-pVDZ	
a'	302, 492, 680, 1308
a''	441, 1001
CCl_2F (Cs) at MP2(fc)/cc-pVDZ	
a'	289, 480, 648, 1199
a''	386, 937

examine the effect of electron correlation. The result is also shown in Fig. 5. One of the C–Cl distances was calculated to be 2.396 Å, which is much smaller than the HF value. The other two C–Cl distances optimized at the MP2 level, on the other hand, were slightly larger than those at the HF level. Harmonic vibrational frequencies calculated at the MP2(fc)/cc-pVDZ level of theory are included in Table 1. The results clearly indicate that the elongated CCl_3F^- structure optimized at the MP2 level has a slightly tighter structure than that at the HF level. This implies that electron correlation in the CCl_3F^- anion is more significant than that in the CCl_3F^+ cation. Although the ab initio direct dynamics calculations are carried out at the HF level of theory in this work, as will be described below, a correlated wave function should be employed in the dynamics calculations in order to obtain more quantitative information.

Fig. 6 shows the schematic description of the vertical electron attachment process for the CCl_3F molecule. The potential energy curves calculated at the HF/cc-pVDZ level of theory are plotted as a function of the C–Cl distance. The solid line represents the potential curve for the neutral CCl_3F molecule. The lower dashed line indicates the potential curve in which the other geometrical parameters are optimized, while the upper dashed line shows the potential curves in which the other geometrical parameters are fixed to those of the neutral CCl_3F molecule. The comparison of these two curves indicates that the effect of geometry optimization is more significant in the Franck–Condon region. This means that the molecular structure is quite different between the optimized CCl_3F^- anion and neutral CCl_3F molecule. On the contrary, the two potential curves are close in energy at longer C–Cl distances, indicating that the effect of geometry optimization is less important.

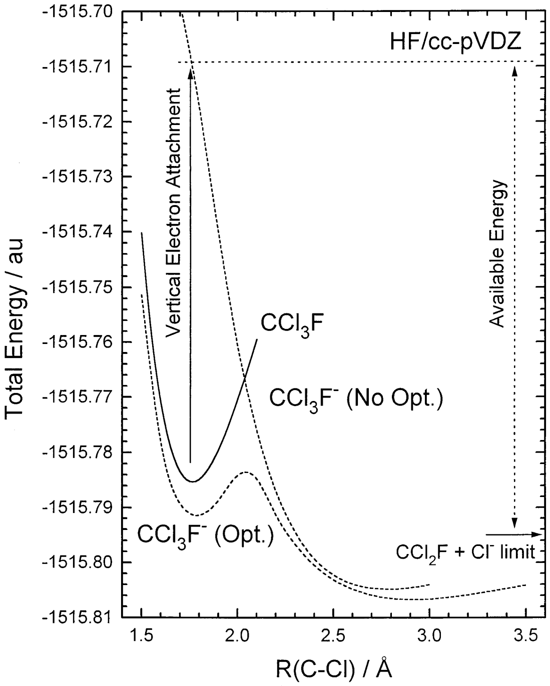

Fig. 6. A schematic description of vertical electron attachment of CCl_3F. Potential curves are calculated at the HF/cc-pVDZ level. “Opt” means that the internal coordinates other than the one C–Cl distance are optimized. “No opt” means that the internal coordinates other than the one C–Cl distance are fixed to those of the neutral CCl_3F minimum.

It is expected from Fig. 6 that vertical electron attachment to the neutral CCl_3F molecule should lead to spontaneous dissociation of the CCl_3F^- anion into CCl_2F and Cl^-. In addition, the available energy would initially be partitioned into the vibrational energy of the CCl_3F^- anion because the effect of geometry optimization may be significant. This behavior is highly contrast to the CCl_3F^+ case. It should be mentioned, however, that the classical trajectory calculations on anions produced by vertical electron attachment must be viewed with caution. As shown in Fig. 6, the total electronic energy of the CCl_3F^- anion with the neutral CCl_3F structure is much larger than that of the neutral molecule. This means that an excess electron is not bound to CCl_3F if the neutral molecule is in its optimized structure. The CCl_3F^- anion produced via electron attachment is initially temporal and again may release the electron within a finite lifetime. If such a lifetime is, however, long enough, the CCl_3F^- anion would change its structure to a more stable structure for which the electronic energy of the anion is lower than that of the neutral molecule. Alternatively, the potential curve for the CCl_3F^- anion in the Franck–Condon region is not a true potential curve but should have a finite energy width. It should be emphasized that the classical trajectory calculations on anions presented in this work completely ignore the electron detachment process, anion → neutral + electron.

The ab initio direct dynamics calculations were carried out under the assumption of vertical electron attachment. A total of 5 trajectories were run and all the trajectory calculations gave essentially the same results. The result of the sample trajectory is plotted in Fig. 7. Fig. 7(a) shows the potential energy as a function of reaction time, while the nuclear distances are plotted as a function of time in Fig. 7(b). It is seen that the potential energy suddenly decreases in a very short time region 0–0.02 ps, suggesting that the potential energy surface in this region is strongly repulsive, although the change in nuclear distances is relatively small. After that, the potential energy suddenly increases and becomes approximately constant. On the other hand, one of the C–Cl distances gradually and monotonously increases. This behavior implies that vertical electron attachment leads to dissociation of CCl_3F^- into the $CCl_2F + Cl^-$ channel. The available energy for this process was calculated to be 54 kcal/mol from Fig. 6 and the relative translational energy between CCl_2F and Cl^- was estimated to be 13 kcal/mol from this trajectory result. This means that 24% of the available energy is partitioned into the relative translational energy and 76% is partitioned into mostly the vibrational energy of the CCl_2F fragment. This result is contrast to the dissociation dynamics of CCl_3F^+, for which most of the available energy is partitioned into the relative translational energy.

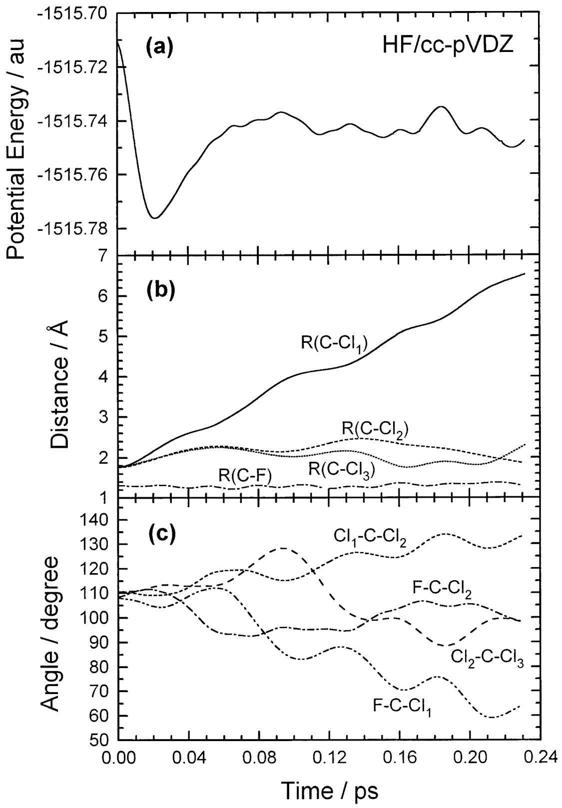

Fig. 7. The result of the classical trajectory calculation for CCl_3F^- formed by vertical electron attachment: (a) potential energy, (b) internuclear distances, and (c) bending angles as a function of time.

The translational energy distribution for the $CCl_3F^- \rightarrow CC_2F + Cl^-$ reaction has experimentally been measured by Dunning and his co-workers [20,21]. They have produced the negative parent ion of CCl_3F by electron transfer reaction, $K^* + CCl_3F \rightarrow K^+ + CCl_3F^-$, where K^* is a potassium atom excited to a high-lying Rydberg state. They have found that the observed translational release is in good agreement with the prediction of statistical theory [19]. Note, however, that the excess energy of the parent ion is very small in their experimental condition and that direct comparison of the present theoretical calculations with the experimental result cannot be possible. Since the present trajectory results show that the dissociation dynamics of CCl_3F^- for large excess energy cannot be described by statistical theory, it would be interesting to measure the energy distributions of the fragments for larger excess energy conditions.

The present trajectory results for CCl_3F^- are also contrast to the trajectory results of CCl_4^-, for which dissociation into $CCl_3 + Cl^-$ did not occur within 0.6 ps [9]. This difference in the dynamics is primarily attributed to the difference in the potential energy curve. As shown in Fig. 4, the potential well for the elongated CCl_3F^- anion was found to be very shallow at the HF/cc-pVDZ level. The direct ab initio dynamics calculations were actually carried out at this level of theory. It can be concluded that the potential well corresponding to the elongated CCl_4^- structure is not shallow to cause a direct dissociation. However, as mentioned before, we found that the inclusion of electron correlation makes the potential well for the elongated CCl_3F^- anion slightly deep. Thus, ab initio direct dynamics calculations using a correlated wave function should be performed in the future in order to obtain more quantitative results. Such a calculation is currently undertaken in our laboratory.

4. Conclusions and future work

In this paper we have applied the ab initio direct dynamics method to the ionization and electron attachment processes for the CCl_3F molecule. Both the CCl_3F^+ and CCl_3F^- ions produced via these processes spontaneously dissociate into $CCl_2F^+ + Cl$ and $CCl_2 + Cl^-$, respectively, within a very short time. In the case of CCl_3F^+ most of the available energy was distributed into the relative translational energy, while most of the available energy was partitioned into the internal vibrational energy of CCl_2F in the case of CCl_3F^-. This essential difference in the dissociation dynamics has been discussed on the basis of the difference in the potential energy curve as a function the C–Cl distance.

We have demonstrated that the ab initio direct dynamics method gives important information which cannot generally be obtained from usual potential energy surface calculations and/or stationary point calculations. The classical trajectory calculations were initiated from the neutral geometry. This means that the direct dynamics method enables us to theoretically simulate the ionization and electron attachment processes of neutral molecules. Therefore, the direct dynamics method can be applied to simulate dissociation channels of larger polyatomic molecular ions, for which potential energy surface calculations would be extremely difficult.

In this work we have considered only the ionization or electron attachment process in the gas phase. However, it may be possible to simulate such a process in condensed phase using the following approximate procedure. Consider an ionization process of a neutral molecule in a rare gas cluster. The interactions between the rare gas atoms can be well approximated using the Lennard-Jones potential functions since many-body interactions are expected to be very small. Also, the interactions between the atoms in the target molecule and the surrounding rare gas atoms may be approximated with the Lennard-Jones potentials. Only for the target molecule the ab initio MO method would be employed. This approximate procedure may probably make actual computations feasible because the use of the ab initio method for all the atoms included in the system will practically be prohibitive. Such a theoretical simulation is currently undertaken in our laboratory.

References

[1] T. Helgaker, E. Uggerud, H.J.A. Jensen, Chem. Phys. Lett. 173 (1990) 145.
[2] E. Uggerud, T. Helgaker, J. Am. Chem. Soc. 114 (1992) 4265.
[3] S.M. Braten, T. Helgaker, E. Uggerud, T. Vulpius, Org. Mass Spectrom. 28 (1993) 1262.
[4] W. Chen, W.L. Hase, H.B. Schlegel, Chem. Phys. Lett. 228 (1994) 436.
[5] T. Takayanagi, A. Yokoyama, Bull. Chem. Soc. Jpn. 68 (1995) 2245.
[6] T. Taketsugu, M.S. Gordon, J. Phys. Chem. 99 (1995) 8642.
[7] T. Taketsugu, M.S. Gordon, J. Phys. Chem. 99 (1995) 14597.

[8] H.-H. Bueker, T. Helgaker, K. Rudd, E. Uggerud, J. Phys. Chem. 100 (1996) 15388.

[9] H. Tachikawa, J. Phys. Chem. 101 (1997) 7454.

[10] H. Tachikawa, K. Komaguchi, Int. J. Mass Spectrom. Ion Processes 164 (1997) 39.

[11] E.L. Øiestad, E. Uggerud, Int. J. Mass Spectrom. Ion Processes 165/166 (1997) 39.

[12] K. Rudd, T. Helgaker, E. Uggerud, J. Mol. Struct. (THEOCHEM) 393 (1997) 59.

[13] S.D. Peyerimhoff, R.J. Buenker, Chem. Phys. Lett. 65 (1979) 434.

[14] M.-B. Huang, S. Lunell, L. Karlsson, Chem. Phys. Lett. 171 (1990) 265.

[15] J.M. Ajello, W.T. Huntress Jr., P. Rayermann, J. Chem. Phys. 64 (1976) 4746.

[16] G.L. Gustev, J. Chem. Phys. 98 (1993) 7072.

[17] M.J. Frisch, G.W. Trucks, H.B. Schlegel, P.M.W. Gill, B.G. Johnson, M.A. Robb, J.R. Cheeseman, T. Keith, G.A. Petersson, J.A. Montgomery, K. Raghavachari, M.A. Al-Laham, V.G. Zakrzewski, J.V. Ortiz, J.B. Foresman, J. Cioslowski, B.B. Stefanov, A. Nanayakkara, M. Challacombe, C.Y. Peng, P.Y. Ayala, W. Chen, M.W. Wong, J.L. Andres, E.S. Replogle, R. Gomperts, R.L. Martin, D.J. Fox, J.S. Binkley, D.J. Defrees, J. Baker, J.P. Stewart, M. Head-Gordon, C. Gonzalez, J.A. Pople, Gaussian 94, Revision D.3, Gaussian, Inc., Pittsburgh, PA, 1995.

[18] T.H. Dunning Jr., J. Chem. Phys. 90 (1989) 1007.

[19] Gas Phase Ion Chemistry, M.T. Bowers (Ed), Academic, London, 1979.

[20] C.W. Walter, K.A. Smith, F.B. Dunning, J. Chem. Phys. 90 (1989) 1652.

[21] C.D. Finch, R. Parthasarathy, H.C. Akpati, P. Nordlander, F.B. Dunning, J. Chem. Phys. 106 (1997) 9594.